

Bumpless SPHERE LQG tip/tilt control with the control switching adaptor

Henri-François Raynaud^a, Hadrien Desvage^a, Caroline Kulcsár^a, Rémi Juvénal^{a,b}, and Cyril Petit^b

^aLaboratoire Charles Fabry, Institut d’Optique Graduate School, France

^bONERA – The French Aerospace Lab

ABSTRACT

The high-performance LQG tip and tilt controller implemented on the SPHERE AO system relies on a stochastic disturbance model of the combined effects of atmospheric turbulence, vibrations and windshake. Model parameters are periodically re-identified from AO telemetry and the controller is re-tuned accordingly.¹ This modus operandi involves frequent updates of the controller while keeping the AO loop engaged. Because LQG is implemented in so-called state-space form, control switching is performed by simply loading new matrices and resetting the controller state (or a part of it) to zero. This results in possibly large transient bumps in both the control and residual phase trajectories. In a previous contribution,² we proposed to mitigate these bumps by resetting the controller state to an appropriate non-zero value, which could be computed recursively by an additional RTC device called the control switching adapter. In this contribution, we introduce an improved implementation of the adapter with reduced computational complexity, and we evaluate its performance using SPHERE on-sky data. The results confirm that the adapter, when properly tuned, is indeed capable of effectively mitigating the amplitude of the bumps.

Keywords: adaptive optics, astronomy, LQG, controller switching, state-space models, Kalman filter

1. WHY CONTROL BUMPS MATTER

In recent years, high-performance Linear Quadratic Gaussian (LQG) tip/tilt controllers have been deployed on or tested for several eXtreme AO (XAO) systems. LQG tip/tilt has thus been successfully implemented on the SPHERE instrument since its first operational deployment in May 2014.^{1,3} More recently, tip/tilt LQG controllers have been extensively tested in “replay mode” simulations based on on-sky data for the the Gemini Multi-Conjugate Adaptive Optics System (Gemini MCAO a.k.a. GeMS)⁴ and for the Subaru Coronagraphic Extreme Adaptive Optics (SCEXAO),⁵ demonstrating in both cases a potential for significant performance improvement over standard integral control.

LQG tip/tilt controllers rely on a minimum-variance prediction of the disturbance (in this case, the combined effects of atmospheric turbulence, wind-shake and vibrations). Prediction is performed by a Kalman filter, which is itself derived from an underlying stochastic model of the disturbance. To achieve and maintain high performance over long observation time, these disturbance models need to be periodically re-identified off-line from recorded wavefront sensor (WFS) measurements, allowing to regularly re-tune the controller. Typical AO runs thus require frequent switching between different LQG controllers (every 30 seconds or so for SPHERE), but also between integrator and LQG (since the AO loop is usually closed first using an integrator).

Switching between different controllers while the AO loop remains closed tends to create transient “control bumps” which degrade performance and may even trigger a cascade of destabilizing effets. In the worst possible scenario, these bumps may propel the guide star spots out of effective range of the WFS camera, causing loss of WFS signal. On-sky implementation of LQG AO control therefore requires efficient bump mitigation mechanisms.

Corresponding author: H.-F. Raynaud, IOGS, 2 av. Augustin Fresnel, 91127 Palaiseau cedex, France
E-mail: henri-francois.raynaud@institutoptique.fr, Telephone: +33 1 64 53 32 62

2. LQG CONTROL BUMPS AND CONTROLLER STATE RESET

LQG control is implemented in real time in so-called state-space form, which involve at each iteration several matrix-vector multiplications. While different state-space forms can and have been used for real-time LQG AO implementation, they are ultimately equivalent to the standard form

$$x_R(k) = A_R x_R(k-1) + B_R y(k), \quad (1)$$

$$u(k) = C_R x_R(k) \quad (2)$$

where $y(k)$ and $u(k)$ denote respectively the WFS measurement and DM control at time $t = kT_s$, and $F_s = 1/T_s$ is the loop sampling frequency. A major benefit of such a state-space implementation is its inherent flexibility: once this generic structure has been coded into the RTC, any linear controller can be implemented by simply loading into memory the appropriate set of matrices (A_R, B_R, C_R) . However, because at time step $t = kT_s$ the RTC uses $x_R(k-1)$ to implement the update equation (1), the RTC memory also needs to store this previous value of the controller state.

When a new set of controller matrices is loaded in at switch time $t = kT_s$, the new control matrices will thus no longer match the current value of $x_R(k_S - 1)$, and this mismatch will cause a transient ‘‘bump’’ in the control u . Furthermore, simply retaining the previous value is not even feasible when the dimension of the controller state changes. The other ‘‘simple stupid’’ choice is to reset $x_R(k_S - 1)$ to zero. Obviously enough, this is likely to generate an even bumpier transient.

The bump mitigation procedures implemented so far on the SPHERE system take advantage of the special structure of the underlying disturbance model, which is the sum of independent second-order stochastic processes – the first of these second-order process models the slowly evolving part of the disturbance (atmospheric turbulence plus wind-shake), the others the vibrations.⁷ As it happens, the dynamics of the turbulence plus windshake part of the model, which corresponds to the two first coordinates of x_R , and hence the corresponding controller gains tend not to change too much when the model is re-identified. Thus, resetting to zero all but the two first coordinates of x_R is a simple yet reasonably effective bump mitigation strategy for the ‘‘LQG to LQG’’ case.

Likewise, while a tip-tilt LQG controller operating in closed-loop is likely to be unstable, it contains a Kalman filter which is guaranteed to be stable. An effective way to ensure bumpless ‘‘integrator to LQG’’ switching is thus to turn on the Kalman filter prior to the switching instant and to let it converge to its steady-state stochastic regime.

However, general-purpose bump mitigation methods are clearly required when the old and new controllers have different internal structures and dynamics. This is the case when the LQG controller is based on a disturbance model with a flexible structure.^{4,5}

3. HOW TO RESET CONTROLLER STATE TO ENSURE BUMPLESS SWITCHING?

3.1 Stitching control trajectories together before switch time

The standard way to achieve bumpless switching to be found in control engineering handbooks is to turn the new ‘‘latent’’ controller on before switching at some time $t_S - t_H = (k_S - n_H)T_s$ and with a zero initial internal state ($x_R(k_S - n_H) = 0$). The latent controller will run in parallel with the active one for $t_S - t_H \leq t < t_S$ time span $t_H = n_H T_s$. During this time, an appropriate feedback signal is added to y in (1-2), in order to force the output of the latent controller to track the control sequence u actually sent to the plant.⁶ This feedback thus drives the controller internal state to a value $x_R(k_S - 1)$ which, so to speak, ‘‘stitches’’ together the virtual control trajectory and the actual one generated by the active controller.

In this paper, we follow the alternative procedure proposed in a previous contribution,² which is to perform this ‘‘trajectory stitching’’ virtually, based on the following observations:

1. When the controller (1-2) is turned on from some non-zero initial state $x_R(k_S - n_H)$ and fed with actual measurements y over the horizon $t_S - t_H \leq t < t_S$, it produces a virtual control trajectory $u_V(k_S - n_H), \dots, u_V(k_S - 1)$ and a final controller state $x_R(k_S - 1)$.

2. Both $u_V(k_S - n_H), \dots, u_V(k_S - 1)$ and $x_R(k_S - 1)$ are linear functions of $x_R(k_S - n_H)$.

As a consequence, the process of determining an optimal value of $x_R(k_S - 1)$ can be formulated and solved off-line, so that this optimal value $x_{R,\text{opt}}(k_S - 1)$ can ultimately be expressed as a linear function of the control and measurement sequences over the “stitching horizon” $t_S - t_H \leq t < t_S$. Furthermore, if this optimization is performed according to a quadratic best-fit criterion, the solution boils down to a simple least-squares orthogonal projection.

3.2 Adapter construction and (low-cost) implementation

In order to determine the value of $x_R(k_S - 1)$ which should be loaded into the RTC together with the new controller matrices, we start from the measurement and control sequences recorded over the stitching horizon, *i.e.* $y(k_S - n_H + 1), \dots, y(k_S - 1)$, $u(k_S - n_H), \dots, u(k_S - 1)$, and look for the optimal value of $x_R(k_S - n_H)$ which minimizes the stitching criterion:

$$J = \sum_{k=k_S-n_H}^{k_S-1} \|u(k) - u_V(k)\|^2 + x_R^T(k_S - n_H) Q x_R(k_S - n_H), \quad (3)$$

with $Q > 0$. The next step is to feed this optimal value of $x_R(k_S - n_H)$ and the measurement sequence $y(k_S - n_H + 1), \dots, y(k_S - 1)$ into (1-2). This yields the desired optimal controller state value $x_{R,\text{opt}}(k_S - 1)$.

As noted above, since the controller is linear, it is immediately checked that at the end of the day the optimal controller state $x_{R,\text{opt}}(k_S - 1)$ is a linear function of the control and measurement sequences $y(k_S - n_H + 1), \dots, y(k_S - 1)$ and $u(k_S - n_H), \dots, u(k_S - 1)$. In other words, there exists two matrices M_u and M_y such that:

$$x_{R,\text{opt}}(k_S - 1) = M_u \begin{pmatrix} u(k_S - 1) \\ u(k_S - 2) \\ \vdots \\ u(k_S - n_H) \end{pmatrix} + M_y \begin{pmatrix} y(k_S - 1) \\ \vdots \\ y(k_S - n_H + 1) \end{pmatrix}. \quad (4)$$

The computation of M_u and M_y involves routine matrix algebra, and the only critical step is to invert the matrix $\Gamma_o(n_H) + Q$, where

$$\Gamma_o(n_H) = \sum_{k=0}^{n_H-1} (A_R^T)^k C_R^T C_R A_R^k \quad (5)$$

is the partial observability Gramian of the pair (A_R, C_R) over the horizon $0 \leq k \leq n_H$.

Equation (4) is an improved version of the control switching adapter introduced in,² with significantly lower real-time computational cost. As it turns out, implementing this streamlined adapter in real time simply requires two FIFO buffers (to store delayed values of u et y over the stitching horizon), and two matrix-vector multiplications at switch time (to compute $x_{R,\text{opt}}(k_S - 1)$ from these FIFO buffers). It should also be noted that when the adapter is engaged at some instant $t_S - t_H$, it will keep updating the value of $x_{R,\text{opt}}$ indefinitely, so that in practice the latent controller can be safely switched on at any time $t \geq t_S$.

4. SIMULATING LQG SWITCHING WITH ON-SKY SPHERE TELEMETRY

To validate the capacity of the adapter to ensure bumpless switching for LQG tip-tilt control in realistic applicative conditions, we used 6 sequences of tip and tilt WFS measurements and controls recorded in short succession during the same SPHERE run in November 2014. These 30-second long sequences of closed loop telemetry were recorded with an LQG controller engaged at sampling frequency $F_s = T_s = 1.2$ kHz and in good AO and seeing conditions (guide star of magnitude $\simeq 3.38$; $r_0 \simeq 0.3@500$ nm, wind speed $\simeq 2$ m./sec.; measurement noise variance $\simeq 10^{-8}$ mas²). LQG performance in residual RMS averages over those 6 dataset was $\sigma_{\text{res}}^2 \simeq 2.21$ mas.

Pseudo-Open Loop (POL) WFS sequences were then computed by subtracting from those closed loop measurements the control values delayed by 2 frames. Because the LQG control matrices were not recorded in

SPHERE telemetry, we recomputed new LQG controllers from the POL sequences using the same identification algorithm and with settings similar to the values used in the SPARTA RTC.⁷ We then checked that the LQG tuned from the last previous sequence achieved performance similar to on-sky results (average rms for these 5 tip and tilt sequences was around 1.8 mas).

We then simulated repeated switches to a re-tuned LQG controller with a full reset of x_R to zero (“dumb switching”). As expected, this generated severe transient bumps in both the control and the residual phase, with jumps of up to 100 mas and above. Clearly, this would in practice have a very detrimental effect on AO performance: as it turns out, such a high-amplitude bump every 30 seconds would in this case increase residual rms by 25 percentage points or more!

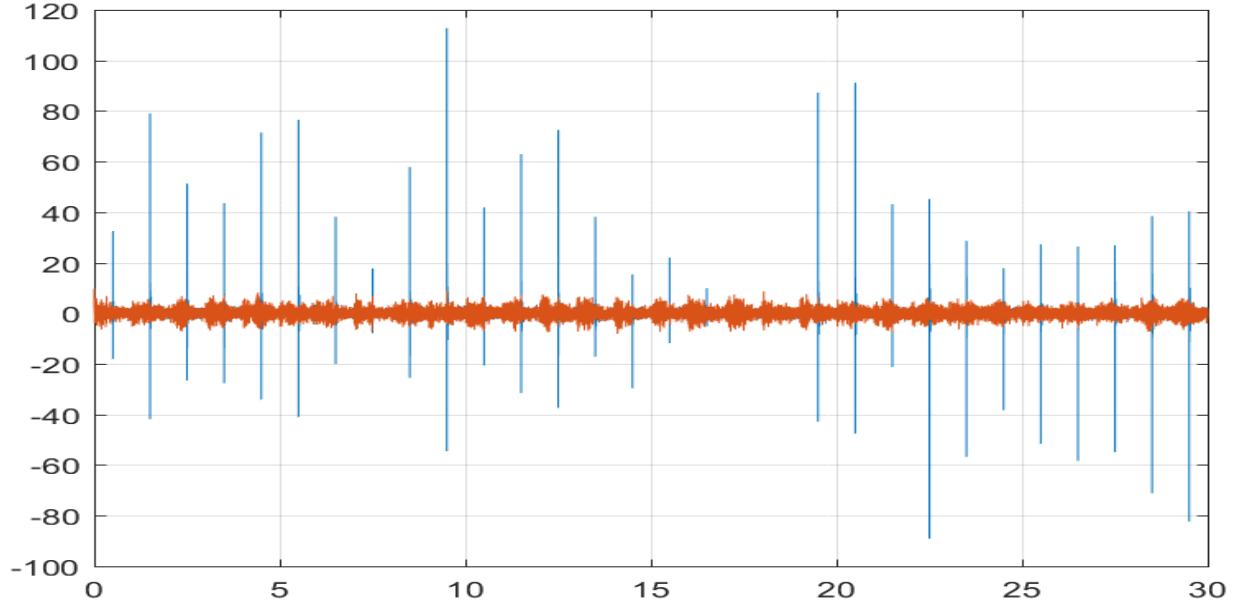


Figure 1. Residual phase trajectories with repeated switching between integrator and LQG for tip sequence #3 without adapter (blue curve) and with adapter (orange curve). Time is in seconds.

5. SIMULATION RESULTS: SWITCHING BETWEEN LQG AND INTEGRATOR WITH AND WITHOUT ADAPTER

We present here simulation results obtained with the tip sequence #3, using the LQG controller tuned from tip sequence #2. Repeated switches between LQG and an integrator (with gain $g = 0.4$) were simulated every 0.5 seconds with and without adapter (*i.e.* with x_R reset to zero). Without switching, the LQG controller achieved significantly higher performance, with $\simeq 1.05$ mas RMS (tip only) vs. $\simeq 2.33$ mas rms for the integrator. (In both cases, the integrator was implemented with the standard bump mitigation procedure for this controller, which is to reset its internal state to the last control value $u(k_S - 1)$.)

Because the identified disturbance model include several poorly damped vibration modes with small variance and with peak frequencies very close to each other, the resulting LQG controller exhibited both weakly observable and weakly controllable modes. As a result, the observability Gramian $\Gamma_o(n_H)$ was poorly conditioned, and the resulting least-squares criterion J required proper regularization. In this particular case, good performance could be achieved by taking:

$$Q = \varepsilon_1 (\Gamma_c(n_H) + \varepsilon_2 I)^{-1}, \quad (6)$$

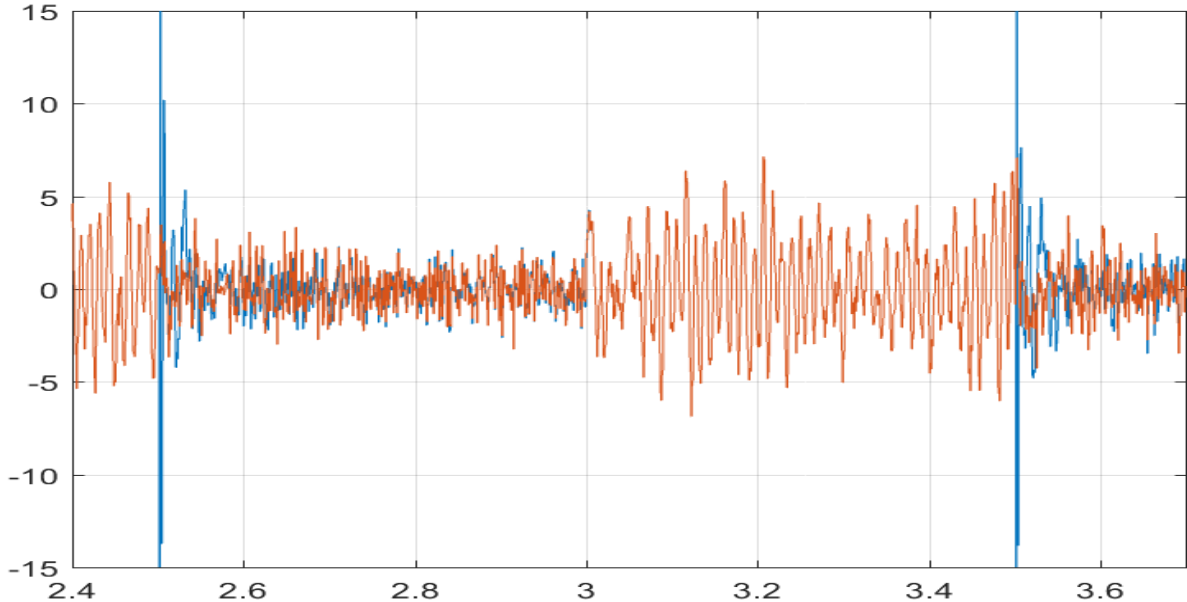


Figure 2. Same curves as in Figure 1, zooming around three successive switching instants: $t_S = 2.5$ (integrator to LQG), $t_S = 3$ (LQG to integrator) and $t_S = 3.5$ (integrator to LQG).

where $\Gamma_c(n_H)$ is the partial controllability Gramian of the pair (A_R, B_R) over the stitching horizon, namely:

$$\Gamma_c(n_H) = \sum_{k=0}^{n_H-1} A_R^k B_R B_R^T (A_R^T)^k. \quad (7)$$

The values of regularization coefficients were $\varepsilon_1 = 10^{-5}$, $\varepsilon_2 = 10^{-12}$. The length of the virtual control trajectory was set to $n_H = 34$, which corresponds to 1.5 times the size of the controller state $n_R = \dim x_R = 23$, and thus to a stitching horizon of $t_H = n_H/F_s \simeq 28$ milliseconds.

Figure 1 shows the simulated residual phase trajectories without adapter (*i.e.* with the controller state x_R reset to zero at each integrator to LQG switch) and with adapter. Figure 2 presents a zoom on these two curves for three successive switches – from integrator to LQG at $t_S = 2.5$ and $t = 3.5$ seconds, from LQG to integrator at $t = 3$ seconds. With the adapter engaged, the control bumps effectively disappear.

6. CONCLUSION

In this paper, we proposed a streamlined implementation of the control switching adapter with low real-time computational cost. Using simulations based on-sky telemetry, we showed that the adapter enables to effectively suppress control bumps for the SPHERE tip-tilt LQG controller. While more complex than existing ad-hoc bump mitigation procedures such as selectively resetting to zero some coordinates of the controller state (as in SPHERE), the adapter is a general purpose method applicable to any controller in state-space form – *i.e.*, to any linear controller. It can thus be used even when the new controller exhibits completely different structure and dynamics, and in both open-loop and closed-loop AO configurations. The adapter is thus not limited to tip-tilt scalar control, but can also be applied to highly multi-variable “full LQG” configurations or to “mixed LQG” control structures (LQG loop for a limited number of low-order optical modes plus integrator or MMSE reconstruction for high-order modes), Fourier-domain LQG or Distributed Kalman filter.

ACKNOWLEDGMENTS

This work has received funding from the European Union’s Horizon 2020 research and innovation programme under grant agreement No 730890.

REFERENCES

- [1] C. Petit, T. Fusco, E. Fedrigo, J.-M. Conan, C. Kulcsár and H.-F. Raynaud, “Optimisation of the control laws for the SPHERE XAO system”, SPIE Conference on Astronomical Telescopes and Instrumentation, 2008.
- [2] H.-F. Raynaud, C. Kulcsár, R. Juvénal, C. Petit, “The control switching adapter: A practical way to ensure bumpless switching between controllers while AO loop is engaged”, SPIE Conference on Astronomical Telescopes and Instrumentation, 2016.
- [3] C. Petit, J.-F. Sauvage, T. Fusco et al., “SPHERE eXtreme AO control scheme: final performance assessment and on sky validation of the first auto-tuned LQG based operational system”, SPIE Conference on Astronomical Telescopes and Instrumentation, 2014.
- [4] L. Leboulleux, G. Sivo et al, “Analysis of GeMS tip-tilt on-sky data: LQG implementation for vibration rejections”, SPIE Conference on Astronomical Telescopes and Instrumentation, 2016.
- [5] J. Lozi, O. Guyon et al, “Characterizing and mitigating vibrations for SCEXAO”, SPIE Conference on Astronomical Telescopes and Instrumentation, 2016.
- [6] W. S. Levine, *The Control Handbook*, IEEE Press, 1996.
- [7] S. Meimon, C. Petit et al., “Tiptilt disturbance model identification for Kalman-based control scheme: application to XAO and ELT systems”, *JOSA A*, **27**(11), pp. A122-A132, 2010.